Electrochimica Acta xxx (2009) xxx–xxx

Contents lists available at ScienceDirect

Electrochimica Acta

journal homepage: www.elsevier.com/locate/electacta

A novel flow battery: A lead acid battery based on an electrolyte with soluble lead(II)—Part VII. Further studies of the lead dioxide positive electrode

Xiaohong Li[a,*], Derek Pletcher[b], Frank C. Walsh[a]

[a] Energy Technology Research Group, School of Engineering Sciences, University of Southampton, Southampton, SO17 1BJ, UK
[b] Electrochemistry and Surface Science Group, School of Chemistry, University of Southampton, Southampton, SO17 1BJ, UK

ARTICLE INFO

Article history:
Received 24 February 2009
Received in revised form 27 March 2009
Accepted 29 March 2009
Available online xxx

Keywords:
Flow battery
Lead acid
Lead dioxide deposition
Methanesulfonic acid
Phase composition

ABSTRACT

Extensive cycling of the soluble lead flow battery has revealed unexpected problems with the reduction of lead dioxide at the positive electrode during discharge. This has led to a more detailed study of the PbO_2/Pb^{2+} couple in methanesulfonic acid. The variation of the phase composition (XRD) and deposit structure (SEM) have been defined as a function of current density, Pb^{2+} and H^+ concentrations, deposition charge and temperature as well as the consequences of charge cycling. Pure α-PbO_2, pure β-PbO_2 and their mixtures can be deposited from methanesulfonic acid media. The α-phase deposits as a more compact, smoother layer, which is well suited to charge cycling. While the anodic deposition of thick layers of PbO_2 is straightforward, their reduction is not; the complexities are explained by an increase in pH within the pores of the deposit. The results suggest that operating the battery at lead(II) concentrations <0.3 M and elevated temperatures should be avoided.

1. Introduction

Earlier papers [1–6] have described results from a programme to develop a soluble lead flow battery for the large-scale storage of energy, for example to act as a buffer between a renewable energy facility and the consumer. The electrolyte is methanesulfonic acid in which lead methanesulfonate has a high solubility (≈2.5 M). Hence the electrode reactions are:

negative electrode

$$Pb^{2+} + 2e^- \rightleftarrows Pb \quad (1)$$

positive electrode

$$Pb^{2+} + 2H_2O \rightleftarrows PbO_2 + 4H^+ + 2e^- \quad (2)$$

and the overall cell reaction

$$2Pb^{2+} + 2H_2O \underset{\text{discharge}}{\overset{\text{charge}}{\rightleftarrows}} Pb + PbO_2 + 4H^+ \quad (3)$$

It should be noted that the electrode chemistries are different from the traditional lead acid batteries in that the electrode reactions do not involve insoluble Pb(II), i.e., lead sulphate within a paste. Moreover, the batteries have quite different characteristics, e.g., the soluble lead acid flow battery can be deep discharged, and the applications envisaged are different. In comparison with other flow batteries, the soluble lead battery has the key advantage that it employs only a single electrolyte and operates without a membrane separator.

We have now carried out extensive charge cycling experiments [7,8]. These have highlighted two problems that limit the battery performance (i) even in the initial cycles, the charge efficiency falls significantly below 100% (typical values are 80–85%) and this leads to build-up of material on both electrodes and (ii) after a number of cycles (typically 20–30, depending on conditions) a black powder appears in the electrolyte and this is lead dioxide detached from the positive electrode surface. This paper sets out to understand these observations.

There is an extensive literature on the electrodeposition of PbO_2 from aqueous solutions [9–15] because of the potential applications of such coatings in electrochemical technology. It is well known that PbO_2 is polymorphic and that the two modifications of α-PbO_2 and β-PbO_2 are well defined. α-PbO_2 has the orthorhombic structure of columbite and β-PbO_2 has the tetragonal, rutile structure. It is also recognised that lead dioxide layers with diverse structures and morphologies can be produced. The literature concerning the preferred conditions for the deposition of a particular structure, morphology or a single polymorph and its purity is, however, confusing and contradictory. In the case of the phase deposited, it is often said that the β-PbO_2 phase is preferably formed in acidic media whereas α-PbO_2 is preferably deposited from alkaline solutions. Even so, quite different results have been reported

* Corresponding author. Tel.: +44 2380 594905.
E-mail address: Xh.Li@soton.ac.uk (X. Li).

0013-4686/$ – see front matter © 2009 Published by Elsevier Ltd.
doi:10.1016/j.electacta.2009.03.075

for deposition from the commonly used acidic nitrate solutions [16–18]. Mindt [19] also reported that a considerable amount of α-PbO_2 appeared in electrodeposits obtained even from concentrated perchloric acid (pH < 0). Similar observations in other acid media have been reported by Duisman and Giauque [20], Thanos and Wabner [21], Munichandraiah [22], and Velichenko et al. [23]. These uncertainties are not surprising since the structure, morphology and phase of PbO_2 deposited depend on several parameters including lead(II) concentration, pH, rate of deposition, the thickness of the deposit, substrate electrode and temperature and these parameters appear to be interactive.

It has also been reported that α-PbO_2 and β-PbO_2 have different properties. For example α-PbO_2 has a more compact crystal morphology. It promotes longer cycle life in the traditional lead acid battery [24], has a higher overpotential for oxygen evolution and presents longer operation time when used as inert anode for ozone generation [25].

We are aware of only a single study of the electrodeposition of PbO_2 from methanesulfonic acid [26]. Under their experimental conditions, Velichenko et al. report the electrodeposition of a mixture of α-PbO_2 and β-PbO_2 with β-PbO_2 being more prevalent and discuss the reaction mechanism in the presence of methanesulfonate ions. There are no detailed reports on the influence of reduction/redeposition cycling on lead dioxide layers.

2. Experimental details

Lead methanesulfonate ($Pb(CH_3SO_3)_2$, Aldrich, 50 wt.%), methanesulfonic acid (CH_3SO_3H, Aldrich, 70 wt.%), lead nitrate ($Pb(NO_3)_2$, BDH, 99%), nitric acid (HNO_3, Fisher, 70%), hexadecyltrimethylammonium hydroxide ($C_{16}H_{33}(CH_3)_3N(OH)$, Fluka, 10 wt.%) were all used as received. All aqueous solutions were freshly prepared with ultra pure water (18 MΩ cm resistivity) from an Elga water purification system.

Cyclic voltammetry was carried out using an Autolab potentiostat/galvanostat PGSTAT30 in a small undivided beaker cell (volume 80 cm^3) equipped with a water jacket connected to a Camlab W14 water thermostat. A carbon/polyvinyl-ester composite electrode (Integris, area 0.2 cm^2), a large area platinum gauze and saturated calomel electrode (SCE) were used as working, counter and reference electrodes, respectively. A fresh sample of carbon/polymer composite was used for each experiment and the back and sides were covered with an insulating tape (polyester tape, Cole-Parmer).

Electrochemical deposition was carried out by the galvanostatic method in the same undivided beaker cell. The cell was fitted with two Integris carbon electrodes, each having a working area of 1 cm × 1 cm (masked with insulating tape), and an inter-electrode gap of 2.0 cm. The cell was stirred with a PTFE coated magnetic stirrer bar (200 rpm). The deposition experiment was also controlled using the Autolab potentiostat/galvanostat PGSTAT30. Some charge/discharge experiments were carried out in the same small undivided beaker cell with two Integris carbon electrodes using an in-house developed, computer controlled charge–discharge and automated logging system. Constant currents were applied and drawn using a dc power supply and load (Thurlby Thandar Instruments, UK). The cell voltage was measured directly using a National Instruments data acquisition system.

The flow cell was custom built in collaboration with C-Tech Innovation Ltd. and has been described elsewhere [7,8]. It was undivided with electrodes having geometric areas of 100 cm^2 (10 cm × 10 cm). The inter-electrode gap was 1.2 cm. For the data reported here, the positive and negative electrodes were Integris carbon and nickel plate, respectively. The electrolyte comprised 0.5 M $Pb(CH_3SO_3)_2$ + 0.5 M CH_3SO_3H + 5 mM $C_{16}H_{33}(CH_3)_3N(OH)$. The additive, $C_{16}H_{33}(CH_3)_3N^+$, is present in the battery electrolyte because of the need to control the structure of the lead deposited at the negative electrode and it is present in this study only because of the desire to use an undivided cell for the battery; its influence on the positive electrode reactions is relatively minor. The electrolyte had a volume of 1500 cm^3, which was circulated through the system by a pump with a mean linear flow velocity of 2.3 cm s^{-1} past the electrode surfaces. The charge/discharge cycling experiment was carried out using the same in-house developed system as described above.

The surface morphology of the PbO_2 samples was obtained using a Philips XL30 or LEO 1455VP scanning electron microscope (SEM) with an accelerating voltage of 15 kV. X-ray diffraction (XRD) data were collected using a Siemens D5000 X-ray diffractometer with Ni-filtered Cu Kα radiation (λ = 1.5406 Å).

3. Results

3.1. Charge/discharge cycling in flow cell

A substantial number of battery cycling experiments has been carried out in an undivided flow cell with 10 cm × 10 cm planar electrodes and using a $Pb(CH_3SO_3)_2 + CH_3SO_3H$ electrolyte also containing the additive, 5 mM $C_{16}H_{33}(CH_3)_3N^+$ added as the hydroxide. Details will be reported elsewhere but a number of observations were pertinent to this study.

(i) The charge efficiency during a series of 2 h charge/discharge cycles at 20 mA cm^{-2} was typically 80–85% if the discharge was terminated after the battery voltage had dropped from approximately 1.5–1.0 V.

(ii) Initially, it was thought that the reason was O_2 evolution at the positive electrode during cell charge. It soon became apparent, however, that a large contributing factor was incomplete reduction of the PbO_2 during discharge. Even after a single charge/discharge cycle, solid material remained on the surface of the electrode. XRD of the deposit showed only lines attributable to PbO_2. The layer appeared still to be compact and adherent as well as no barrier to further deposition during the next charge. Hence, the reduction does not appear to terminate because of loss of electrical contact with the positive electrode.

(iii) After 10–20 cycles, a thick layer of PbO_2 builds up on the positive electrode. This may be stripped off the electrode, dried and weighed and consideration of the mass balance confirms that PbO_2 accumulating on the electrode accounts for a large fraction of the shortfall from 100% charge efficiency.

(iv) The deviation of the charge efficiency from 100% also leads to accumulation of lead on the negative electrode. The accumulation of lead and lead dioxide on the two electrodes leads to a continuous, and eventually significant, fall in the Pb(II) concentration in the electrolyte. Analysis of the Pb(II) in solution together with the weights of Pb on the negative electrode and PbO_2 on the positive electrode accounts for all the Pb(II) in the initial electrolyte.

(v) After a number of charge/discharge cycles, the PbO_2 layer becomes less compact and black particulate material appears in the electrolyte. This may take >30 cycles and does not necessarily lead to immediate failure of the battery; the battery may continue to cycle but it is clearly not a desirable process.

(vi) The first appearance of the black powder occurs during discharge and the powder content of the electrolyte builds up on subsequent cycles.

(vii) The cycle life of the battery can be extended significantly by periodic addition of $Pb(CH_3SO_3)_2$ to replace the Pb(II) lost

Please cite this article in press as: X. Li, et al., A novel flow battery: A lead acid battery based on an electrolyte with soluble lead(II)—Part VII. Further studies of the lead dioxide positive electrode, Electrochim. Acta (2009), doi:10.1016/j.electacta.2009.03.075

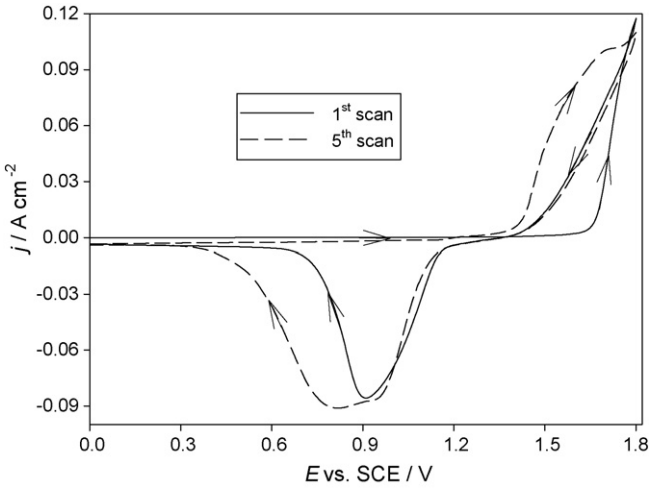

Fig. 1. Cyclic voltammograms recorded at a carbon/polyvinyl-ester composite electrode (area 0.2 cm^2) in an electrolyte solution containing 0.5 M $Pb(CH_3SO_3)_2$ + 0.5 M CH_3SO_3H. The first and fifth scans are shown. Potential sweep rate: 20 mV s^{-1}. Temperature: 298 K.

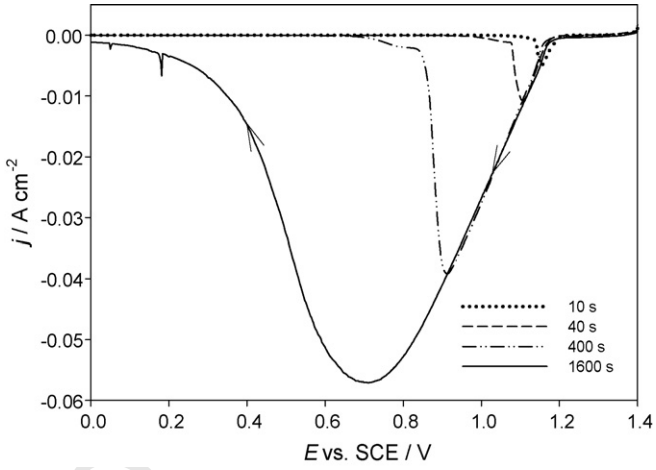

Fig. 2. Linear sweep voltammograms recorded at a carbon/polyvinyl-ester composite electrode (area 1 cm^2) in an electrolyte solution containing 0.5 M $Pb(CH_3SO_3)_2$ + 0.5 M CH_3SO_3H. Before each sweep a thin layer of PbO_2 was deposited at a constant current density of 20 mA cm^{-2} at electrode for 10, 40, 400, and 1600 s, respectively. Potential sweep rate: 1 mV s^{-1}. Temperature: 298 K.

as Pb and PbO_2 onto the negative and positive electrodes, respectively.

3.2. Voltammetric studies

Fig. 1 shows cyclic voltammograms (potential scan rate 20 mV s^{-1}) recorded at a fresh piece of carbon/polyvinyl-ester composite electrode (area 0.2 cm^2) in a solution containing 0.5 M $Pb(CH_3SO_3)_2$ + 0.5 M CH_3SO_3H at 298 K. Also shown is the 5th cycle with no cleaning of the electrode between cycles. The scan to positive potentials during the first cycle shows no current negative to approximately +1.65 V *vs.* SCE followed by a steep rise in anodic current positive to this critical potential. This current leads to the deposition of lead dioxide and this continues until ca. +1.4 V *vs.* SCE on the reverse scan; that is, the voltammogram exhibits a nucleation loop. Reduction of the lead dioxide is seen as a symmetrical cathodic peak centred around +0.90 V and reduction is completed by 0.6 V *vs.* SCE. On subsequent cycles an anodic current is seen at all potentials positive to ca. +1.40 V *vs.* SCE and more PbO_2 is deposited. In consequence, the charge associated with the reduction of the lead dioxide increases. Many similar voltammograms have been reported in the literature. Here, we would like to focus on one feature of the response; as the charge associated with the cathodic reduction of the lead dioxide increases, the cathodic peak broadens significantly and on the fifth cycle, the reduction process is not completed until around. 0.4 V *vs.* SCE. A possible explanation for the peak broadening is that, with a thicker film, the reduction of the PbO_2 leads to a decrease in proton concentration, see reaction (2), within the structure of the layer. This would then lead to a negative shift in the formal potential for the cathodic reduction, given by:

$$E_e = E_e^o + \frac{2.3RT}{2F} \log \frac{[H^+]^4}{[Pb^{2+}]} \quad (4)$$

In fact, the predicted shift is −120 mV for an increase in pH of 1 unit at 298 K.

To test this suggestion, a further set of experiments was carried out with the same composition solution. In these experiments, a layer of PbO_2 was deposited using a constant current density of 20 mA cm^{-2} for various times and the reduction of the layer was then carried out using a slow potential scan (potential scan rate, 1 mV s^{-1}). The aim was to investigate the influence of the deposit thickness on the reduction of the PbO_2 while minimising non-steady state effects. Fig. 2 shows the responses for the reduction of PbO_2 layers with four deposit thicknesses while Table 1 reports data from these voltammograms. It can be seen that in the initial stages of reduction, the response is almost independent of the layer thickness but with increase in the thickness of the PbO_2 layer, the reduction of much of the layer only occurs at much more negative potentials. The peaks become much broader and the current efficiency for the reduction of PbO_2 decreases from >99% to 91.5%. With the thickest deposit, some black material could still be seen on the surface after the experiment. This data is only compatible with a transport limitation within the film. This limitation is most likely the supply of protons and it should also be noted that a substantial rise in pH could even lead to the deposition of hydroxides and oxides of lead such as PbO.

3.3. Phase composition as a function of deposition conditions

A series of depositions was carried out using 1 cm^2 Integris carbon electrodes in the small undivided beaker cell and the phase composition was determined by X-ray diffraction (XRD). The identification of α-PbO_2 and β-PbO_2 was performed by comparison with the ICDD database (α-PbO_2 card no. 72-2440, β-PbO_2 card no. 76-0564) [27]. According to the standard XRD pattern of the two phases, strong diffraction peaks of both phases are present in the range 20–40° (2θ) and the peaks are clearly distinguishable. It should be noted that a quantitative determination of the amount of the two phases is not possible from the X-ray diffractogram, particularly for the thinner film samples which have preferred orientation effects. Fig. 3 illustrates the results, showing typical diffractograms for deposits identified as α-PbO_2, β-PbO_2 and a mixture. The mean

Table 1
Data taken from the reduction of PbO_2 layers of different thicknesses. Deposition at 20 mA cm^{-2}; reduction during a potential scan at 1 mV s^{-1}. All potentials *vs.* SCE. Electrolyte: 0.5 M $Pb(CH_3SO_3)_2$ + 0.5 M CH_3SO_3H, pH 0.45. Electrode: carbon/polyvinyl-ester composite. Temperature: 298 K.

Deposition time (s)	Deposition charge (C cm^{-2})	Peak potential (mV)	Potential at which reduction is complete (mV)	% charge efficiency
10	0.2	1153	1130	99.6
40	0.8	1107	1005	98.1
400	8.0	912	710	96.4
1600	32.0	712	<0	91.5

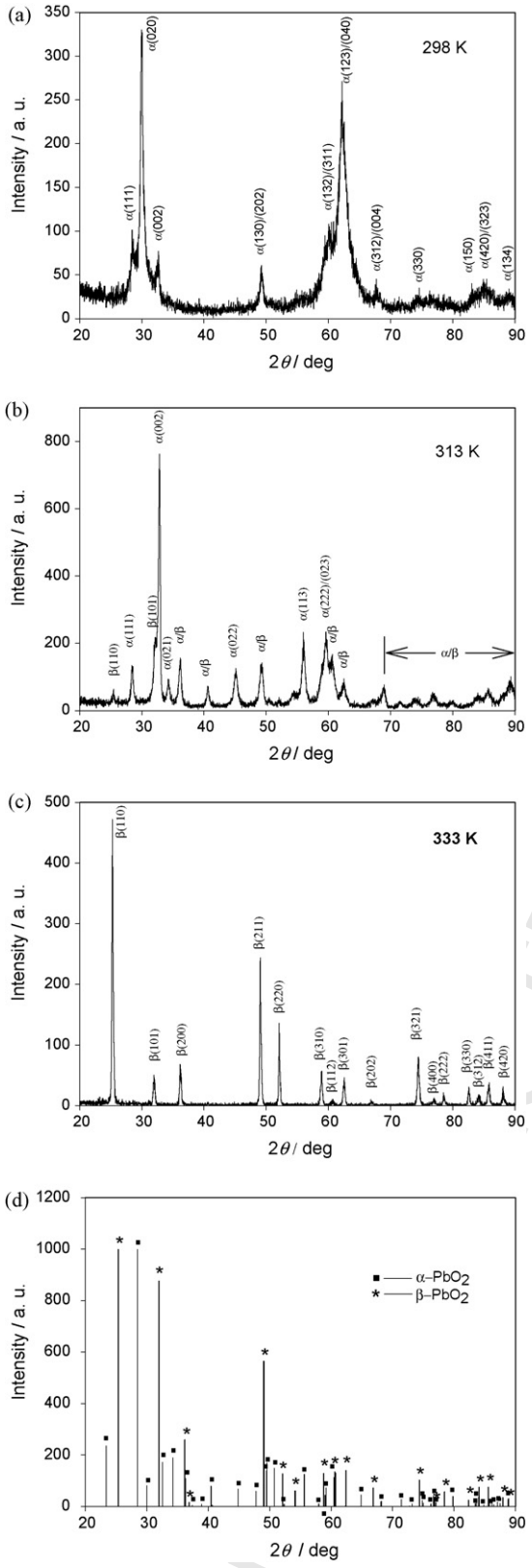

Fig. 3. X-ray diffractograms of PbO_2 films deposited from 0.5 M $Pb(CH_3SO_3)_2$ + 0.5 M CH_3SO_3H at current density of 20 mA cm^{-2} at various temperatures: (a) 298 K, (b) 313 K, and (c) 333 K. The standard XRD patterns of the α-PbO_2 and β-PbO_2 phases are shown in (d).

Table 2
Influence of the current density on the phase composition of PbO_2. Electrolyte: 0.5 M $Pb(CH_3SO_3)_2$ + 0.5 M CH_3SO_3H, pH 0.45. Temperature: 298 K. Electrode: carbon/polyvinyl-ester composite. Deposition time: 2 h (except 120 mA cm^{-2}, where the deposition time was 1 h).

Current density (mA cm^{-2})	Phase composition	Mean grain size (nm)
4	α-PbO_2	19
20	α-PbO_2	18
50	α-PbO_2	17
70	α-PbO_2	18
120	α-PbO_2	23

grain size was estimated from the width of the strongest diffraction peak using the Debye–Sherrer equation [28].

Table 2 shows the influence of current density for a solution of 0.5 M $Pb(CH_3SO_3)_2$ + 0.5 M CH_3SO_3H at 298 K. Current density has little influence of the deposit formed. Although these experiments led to thick deposits (up to 1 mm in thickness), at all current densities the deposits appear compact and uniform by eye; at lower current density, the deposits are shiny and can be highly reflecting [29]. Also, it is always pure α-PbO_2 that is deposited and the grain size is constant. In contrast, temperature has a substantial effect, see Table 3. While pure α-PbO_2 is formed at 298 K, pure β-PbO_2 results from deposition at 348 K and mixtures are formed at intermediate temperatures. There is also a gradation in the mean grain size, rising from 19 to 57 nm with the increase in temperature. Since the acidic nitrate media have been much more extensively studied, two experiments were performed in a nitrate medium. In acidic nitrate electrolytes, the deposition at 298 K led to a mixture of α-PbO_2 and β-PbO_2 and pure β-PbO_2 at 348 K and again an increase in grain size was observed. This trend is in agreement with the literature [21,23]. It is observed in both the nitrate and methanesulfonate media that β-PbO_2 phase exhibits preferential orientation along (1 1 0) plane and the diffraction peaks become well defined at higher temperature. This is also in complete agreement with previous literature [21,23]. It has been suggested that this preferred orientation results from epitaxial growth on the substrate but this seems unlikely when the phenomenon is seen at carbon, platinum and titanium substrates. Alternatively, Thanos and Wabner [21] have proposed that the effect of increased temperature can be attributed to a decrease of the potential for the onset of electrodeposition. At relatively low potentials, the formation of polycrystalline assemblies is less probable and, therefore, disorder effects are less common. Taking into account that the growth rate along different crystallographic directions may depend only slightly on temperature, preferred crystallographic orientations could become more pronounced at higher temperatures mainly due to the fact that the number of the polycrystalline assemblies on the electrode surface is smaller. This explanation is supported by our results and others [23], where the deposition potential is indeed lower at higher temperature and preferred crystallographic orientations are observed at relatively high temperatures.

Table 3
Influence of the temperature on the phase composition of PbO_2. Electrolyte: 0.5 M $Pb(CH_3SO_3)_2$ + 0.5 M CH_3SO_3H, pH 0.45. Current density: 20 mA cm^{-2}. Electrode: carbon/polyvinyl-ester composite. Temperature: 298 K. Deposition time: 2 h. For comparison, two results with the electrolyte, 0.5 M $Pb(NO_3)_2$ + 0.5 M HNO_3, are reported.

Anion	Temperature (K)	Phase composition	Mean grain size (nm)
$CH_3SO_3^-$	298	α	18
$CH_3SO_3^-$	313	α + β	27
$CH_3SO_3^-$	323	α + β	27
$CH_3SO_3^-$	333	β	38
$CH_3SO_3^-$	348	β	57
NO_3^-	298	α + β	32
NO_3^-	348	β	70

Please cite this article in press as: X. Li, et al., A novel flow battery: A lead acid battery based on an electrolyte with soluble lead(II)—Part VII. Further studies of the lead dioxide positive electrode, Electrochim. Acta (2009), doi:10.1016/j.electacta.2009.03.075

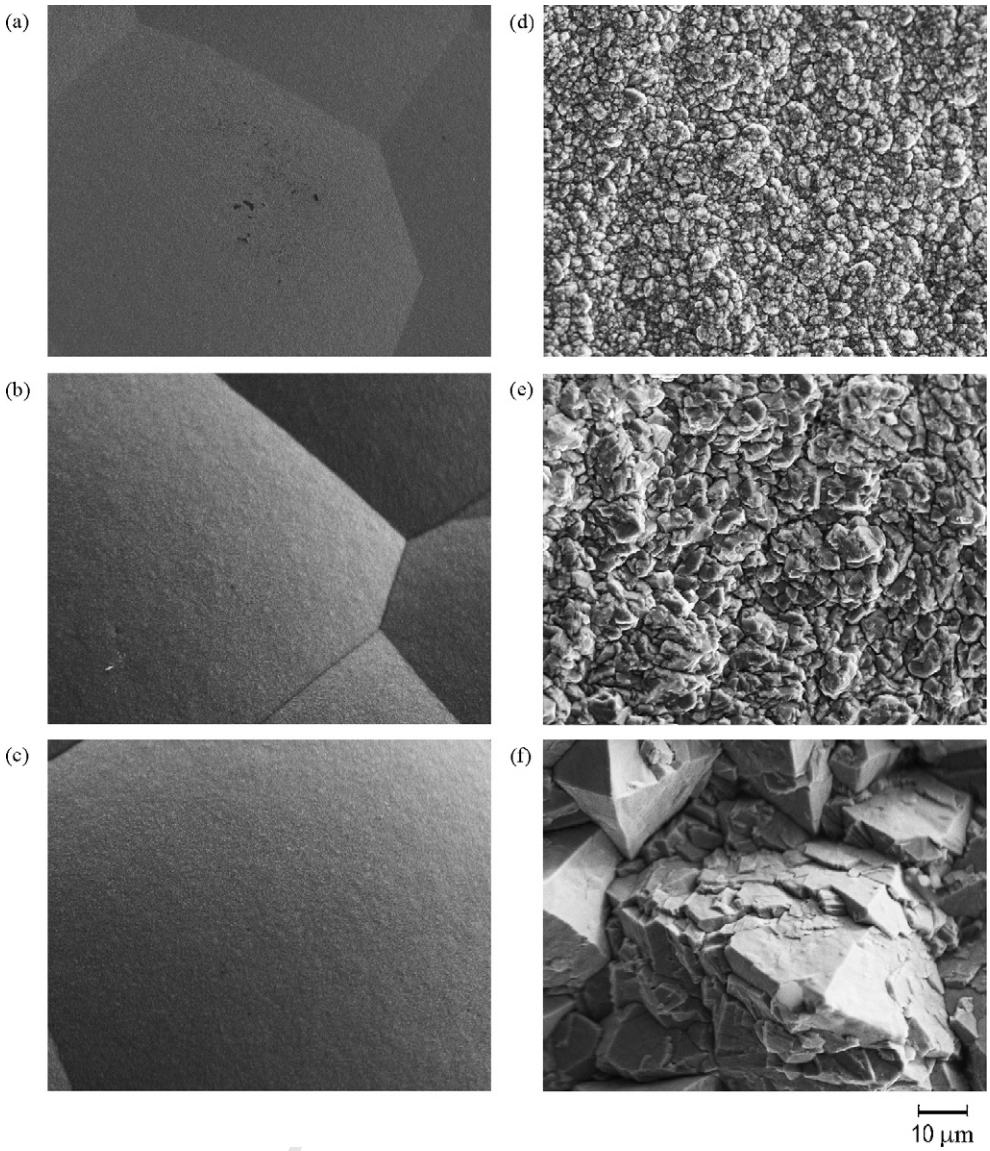

Fig. 4. SEM images of PbO_2 films deposited from an electrolyte containing 0.5 M $Pb(CH_3SO_3)_2$ + 0.5 M CH_3SO_3H at various current densities and temperatures: at 298 K at various current density: (a) 20 mA cm^{-2}, (b) 50 mA cm^{-2}, and (c) 120 mA cm^{-2}; at a current density 20 mA cm^{-2} at various temperature: (d) 313 K, (e) 333 K, and (f) 348 K.

The experiments were then extended to the composition of the electrolyte; both Pb^{2+} and H^+ concentrations were considered, partly because Velichenko et al. [26] reported deposition of β-PbO_2 as the prevalent phase from an acidic methanesulfonate solution. Our results are reported in Table 4. When the deposition was repeated in the same conditions as Velichenko et al., i.e., lower Pb^{2+} concentration, we also found the β-PbO_2 to be the dominant phase. It was also clear that the appearance of the films and their adherence to the substrate electrode depended on the concentration of Pb^{2+} and current density. The trend is to powdery deposits and poor adherence if mass transfer control is approached during deposition. The change from β-PbO_2 to α-PbO_2 with increasing Pb^{2+} concentration is much more surprising but may be associated with a trend to mass transport control at lower Pb^{2+} resulting in the deposition of β-PbO_2.

Table 4
Influence of the Pb^{2+} and H^+ concentrations in methanesulfonate solutions on the phase composition of PbO_2. Electrode: carbon/polyvinyl-ester composite. Temperature: 298 K. Deposition time: 2 h.

Concentration (M)		Current density (mA cm^{-2})	Phase composition	Mean grain size (nm)	Visual appearance
Pb^{2+}	H^+				
0.1	0.1	4	β + trace α	24	Compact
0.1	0.1	20	β	32	Powdery
0.1	0.5	20	β	22	Powdery
0.2	0.5	20	α + β	27	Powdery
0.3	0.5	20	α	23	Compact
0.5	0.5	20	α	18	Compact

3.4. SEM characterisation of deposits

Fig. 4 shows SEM images of deposits from 0.5 M $Pb(CH_3SO_3)_2$ + 0.5 M CH_3SO_3H at various current densities and temperatures. Again, it can be seen that temperature has a much stronger influence and there appears to be a correlation between the surface morphology and the phase composition. At room temperature, and at all current densities, where α-PbO_2 is formed, the deposit appears to be rather flat and made up of features (polygonal in shape) with dimensions several hundred microns in size. At much higher magnification, these features can be seen

Please cite this article in press as: X. Li, et al., A novel flow battery: A lead acid battery based on an electrolyte with soluble lead(II)—Part VII. Further studies of the lead dioxide positive electrode, Electrochim. Acta (2009), doi:10.1016/j.electacta.2009.03.075

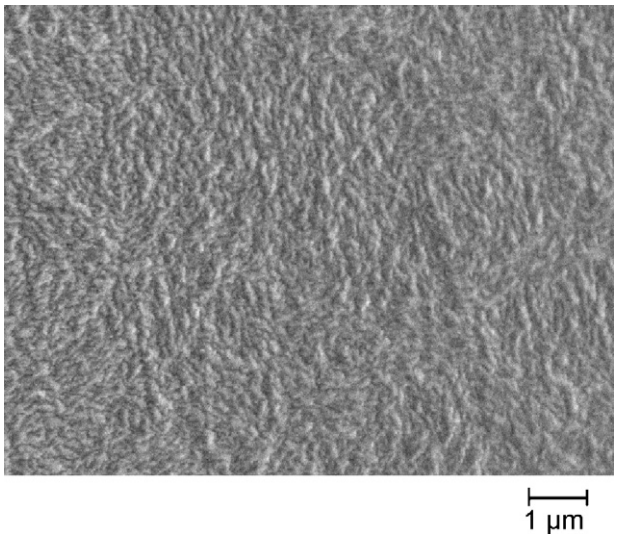

Fig. 5. High magnification SEM image of a PbO_2 film deposited from an electrolyte containing 0.5 M $Pb(CH_3SO_3)_2$ + 0.5 M CH_3SO_3H at current density of 20 mA cm^{-2} at 298 K.

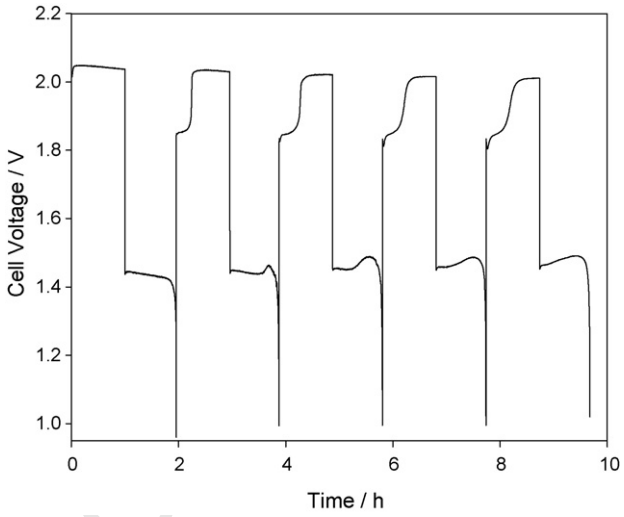

Fig. 6. Cell voltage *vs.* time response for five charge/discharge cycles at current density of 20 mA cm^{-2}. The experiment was carried out with two carbon/polyvinyl-ester composite electrodes in an electrolyte solution containing 0.5 M $Pb(CH_3SO_3)_2$ + 0.5 M CH_3SO_3H with stirring. Inter-electrode gap: 2 cm. Temperature: 298 K.

to be constructed from smaller grains, see Fig. 5. As soon as the temperature is increased so that some β-PbO_2 is deposited, this structure is totally disrupted. At 348 K, where β-PbO_2 is formed as a pure phase, the structure is angular and composed of grains with dimensions <10 μm in size. Both types of SEM image have previously been reported in the literature [21,22,26].

3.5. Charge/discharge cycling in a beaker cell

A series of charge/discharge cycling experiments was carried out in the beaker cell. The electrolyte was again 0.5 M $Pb(CH_3SO_3)_2$ + 0.5 M CH_3SO_3H at pH 0.45. During each cycle, lead dioxide was deposited with a current density of 10 or 20 mA cm^{-2} for 1 h (when the open-circuit potential was +1.76 V) and then discharged with the same current density until the cell voltage dropped to 1.1 V. As in the larger cell, the charge efficiency for the cycles was 80–85%. At the end of the discharge cycle, the open-circuit potential was +1.63 V, another clear indication that PbO_2 remained on the surface of the electrode.

Fig. 6 reports the cell voltage *vs.* time response during the first five cycles of a charge cycling experiment carried out in the beaker cell with a current density of 20 mA cm^{-2}. During the first charge the cell voltage is almost constant at around +2.05 V following an initial rise and then decline that can be associated with nucleation of PbO_2. Discharge occurs close to +1.40 V (note the inter-electrode gap is 2 cm, higher than in the flow cell). On subsequent cycles, the behaviour is more complex during charge; charge commences at +1.85 V and later increases back to around +2.0 V. This behaviour has been seen in all our previous works and has been discussed [1,2]. Monitoring the individual electrode potentials shows that this feature is associated with the positive electrode. It clearly indicates that the conversion of Pb^{2+} in solution to PbO_2 requires the cell voltage to be >2.0 V and that the positive electrode chemistry early in the charge process must be a more facile reaction leading to PbO_2. This can only be the oxidation of a species on the positive electrode surface and formed during the discharge process. We have not been able to identify this species and it does have unique peaks in the XRD over the 2θ range recorded. As this charge cycling was continued some black powder began to form in solution after >30 cycles.

Fig. 7 shows SEM images of the deposit on the positive electrode after completion of 20 cycles and the electrode is discharged. The layer has been fractured such that the cross-section is exposed. Fig. 7(a) shows that it is thick, >200 μm and is made up of a number of well-defined layers. Fig. 7(b) is an image of one of the 'cliffs' on a higher magnification and reveals the compact nature of the layers that are failing to reduce during discharge. XRD shows that a mixture of α-PbO_2 and β-PbO_2 is the major component of this layer. We cannot rule out the presence of, for example, PbO since the diffraction peaks coincide with those of β-PbO_2. Indeed, the cell voltage *vs.* time response during charge cycling can only be explained on the basis of a Pb(II) species in the deposit at discharge. From the SEM images of the surface after cycling, it is clear that the surface is becoming rougher with time; this is illustrated in Fig. 8, images obtained after 2 and 10 cycles.

The phase composition was also monitored during charge cycling and the data are reported in Table 5. At all current densities, it is clear that there is a trend from pure α-PbO_2 in the early charges to a mixture of α-PbO_2 and β-PbO_2 with cycling with the β-PbO_2 becoming apparent after approximately 10 cycles. This β-PbO_2 can be seen both when the electrode is examined in the charged state and when it is examined in the discharged state. It has previously been noted that in sulphuric acid there is also a change in phase

Table 5
Influence of charge cycling on the phase composition of PbO_2. Electrolyte: 0.5 M $Pb(CH_3SO_3)_2$ + 0.5 M CH_3SO_3H, pH 0.45. Electrode: carbon/polyvinyl-ester composite. Temperature: 298 K. Deposition time: 1 h. The same current density was used for charge and discharge. A cycle number of '.5' indicates the charged state or half cycle.

Current density (mA cm^{-2})	Cycle number	Phase composition
10	0.5	α
10	4.5	α
10	5.0	α
10	9.5	α + β
10	10.0	α + β
20	0.5	α
20	2.5	α
20	9.5	α + β
20	19.5	α + β
20	39.5	α + β
20	40.0	α + β
50	0.5	α
50	1.0	α
50	9.5	α + β

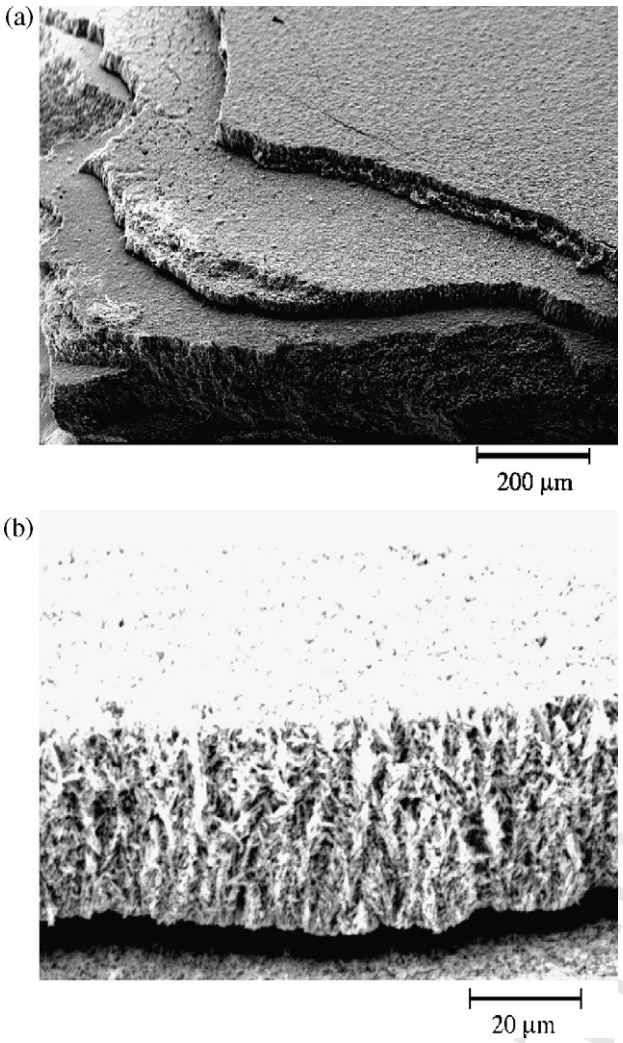

Fig. 7. Cross-sectional SEM images of PbO_2 layers after 20 cycles of charge/discharge at (a) lower magnification and (b) higher magnification. The cell was charged at 20 mA cm^{-2} for 1 h and discharged at the same current density until the voltage dropped to 1.0 V. The experiment was carried out with two carbon/polyvinyl-ester composite electrodes in an electrolyte solution containing 0.5 M $Pb(CH_3SO_3)_2$ + 0.5 M CH_3SO_3H with stirring. Inter-electrode gap: 2 cm. Temperature: 298 K.

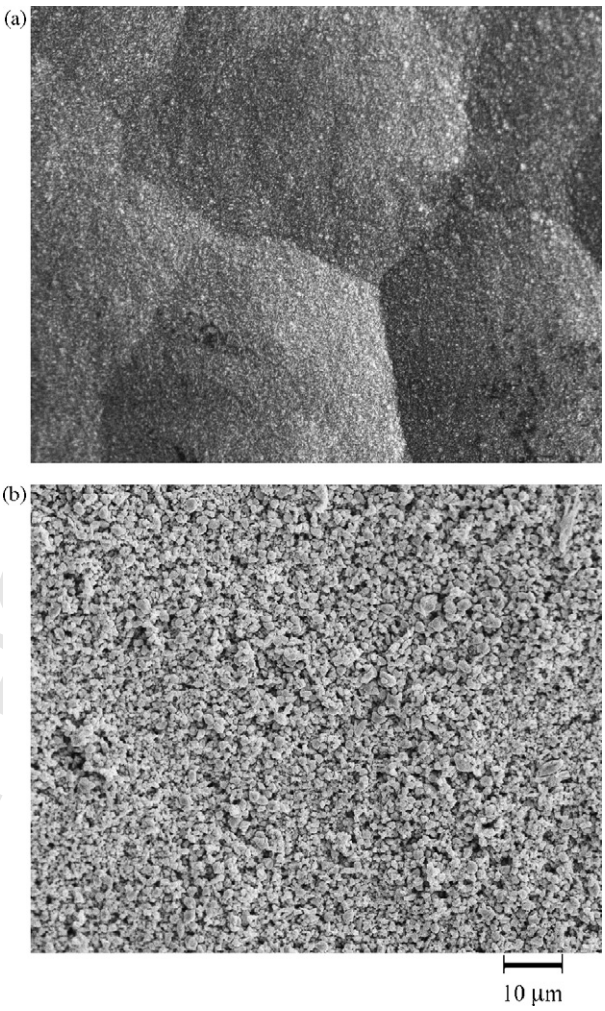

Fig. 8. SEM images of PbO_2 surface after (a) 2 cycles of charge/discharge and (b) 10 cycles of charge/discharge. The cell was charged at 20 mA cm^{-2} for 1 h and discharged at the same current density until the voltage dropped to 1.0 V. The experiment was carried out with two carbon/polyvinyl-ester composite electrodes in an electrolyte solution containing 0.5 M $Pb(CH_3SO_3)_2$ + 0.5 M CH_3SO_3H with stirring. Inter-electrode gap: 2 cm. Temperature: 298 K.

composition of the PbO_2 within the positive electrode paste with cycling [16,17,30–32].

4. Discussion

It is clear that high quality, thick lead dioxide layers can be deposited onto carbon substrates from methanesulfonic acid solutions provided that the lead(II) concentration is sufficiently high. Using an electrolyte containing 0.5 M $Pb(CH_3SO_3)_2$ at room temperature (298 K), it was possible to deposit layers >0.5 mm thick that were compact, smooth and adherent to the surface, even at current densities up to 120 mA cm^{-2}. These deposits are also pure α-PbO_2.

With increasing temperature or a decrease in lead(II) concentration, the picture becomes more complicated. There is a trend to both powdery deposits and the formation of β-PbO_2 with decrease in lead concentration and to the formation of β-PbO_2 with increase in temperature. Mass transport limitations are clearly one influence in the formation of powdery deposits. The different phases could arise from quite different deposition mechanisms. Lead(IV) has a finite solubility in methanesulfonic acid and this will increase with temperature and also be more important at low current densities; hence β-PbO_2 could arise from a dissolution/precipitation mechanism while α-PbO_2 is formed by a more direct deposition process (comparable to the deposition of a metal). Our experiments also show a strong correlation between a very smooth deposit and the formation of pure α-PbO_2 (the structure of Fig. 4(a) is always found with α-PbO_2) and a much rougher and angular surface with β-PbO_2. Although the structure shown by β-PbO_2 is not always associated with loss of compactness and formation of powder, it may well be a precursor in appropriate conditions. It may also be that a mixture α-PbO_2 and β-PbO_2 leads to a less ordered structure in thick layers, with a greater chance of powder deposition.

In contrast to its deposition, the reduction of thick layers of PbO_2 is never straightforward. It is evident that the reduction of thick layers becomes more difficult and shifts to more negative potentials as the deposit is removed. Moreover, in conditions where the reduction is a discharge process in a battery, some of the PbO_2 is not reduced and deposit remains on the surface of the carbon. Although it cannot be proven conclusively, there is good reason to believe that the negative shift in the reduction potential arises because of proton starvation within the PbO_2 as reaction (1) takes place. In our normal charge/discharge regime, where the discharge is terminated at a cell voltage of +1.0 V (a positive electrode potential of

Please cite this article in press as: X. Li, et al., A novel flow battery: A lead acid battery based on an electrolyte with soluble lead(II)—Part VII. Further studies of the lead dioxide positive electrode, Electrochim. Acta (2009), doi:10.1016/j.electacta.2009.03.075

~0.6 V *vs.* SCE), the voltammetry would indicate that a significant amount of the deposit would not be reduced and this is confirmed by visual observation or weighing. The potential *vs.* time response during charge/discharge cycling confirms an earlier observation [2] that the cell voltage *vs.* time response during charge is complex, the cell voltage (and positive electrode potential) increases with time. This would seem to implicate an unidentified lower oxidation state lead species within the deposit after discharge.

The small battery in the beaker cell can be charge/discharge cycled effectively for a number of cycles. A charge efficiency of 90% and a voltage efficiency of 75% can be achieved for more than 20 cycles. After such number of cycles, there is substantial deposit on the positive electrode and the lead dioxide builds up layer by layer and also changes from pure α-PbO_2, to a mixture α-PbO_2 and β-PbO_2 as well as becoming less smooth and compact; eventually powdery deposits are formed. During such experiments, however, there is a substantial build-up of both lead on the negative electrode and lead dioxide on the positive electrode and this leads to a decrease in the Pb^{2+} concentration in solution. The decrease in lead(II) concentration contributes markedly to these changes.

5. Conclusions

It is possible to deposit thick layers of pure α-PbO_2, pure β-PbO_2 and their mixtures from methanesulfonic acid solutions and confirmed that the phase formed depends on a number of experimental parameters. The deposits of both α-PbO_2 and β-PbO_2 can be compact and adherent if the conditions are selected correctly. It has also demonstrated that the deposition of PbO_2 is a straightforward process compared to its reduction process. The reduction requires an increasingly negative potential during the reduction of thick layers and, in general, not all the PbO_2 layer is reduced. Indeed, it is the difficulties associated with the reduction of PbO_2 that leads to the problems during battery cycling; it is the major cause of the charge imbalance during charge/discharge cycles and eventually leads to shedding of the lead dioxide into solution.

Because of the trend to form rough and/or powdery deposits at lower lead(II) concentrations and higher temperatures, the soluble lead acid flow battery should be operated close to room temperature and the lead concentration should be maintained above 0.3 M. Indeed, it appears that the battery performs best in conditions where only α-PbO_2 is formed. There appears to be no way to avoid the overpotentials associated with both the charge and discharge reactions at the positive electrode and also the build-up of lead and lead dioxide on the electrodes appears inevitable. We will, however, later report regimes where the battery can be cycled extensively [8]. Avoidance of PbO_2 shedding from the surface requires tight control of the battery electrolyte and flow conditions during cycling.

Acknowledgements

The authors are grateful for financial support via a DTI Technology Programme (Contract TP/4/EET/6/I/2296) entitled '*Redox Flow Cells for Intelligent Grid Management*'. They also acknowledge the support of the partners in this programme, C-Tech Innovation Ltd. (J. Collins and D. Stratton-Campbell) and E-ON UK Ltd. (J. Bateman).

References

[1] A. Hazza, D. Pletcher, R. Wills, Phys. Chem. Chem. Phys. 6 (2004) 1773.
[2] D. Pletcher, R. Wills, Phys. Chem. Chem. Phys. 6 (2004) 1779.
[3] D. Pletcher, R. Wills, J. Power Sources 149 (2005) 96.
[4] A. Hazza, D. Pletcher, R. Wills, J. Power Sources 149 (2005) 103.
[5] D. Pletcher, H. Zhou, G. Kear, C.T.J. Low, F.C. Walsh, R. Wills, J. Power Sources 180 (2008) 621.
[6] D. Pletcher, H. Zhou, G. Kear, C.T.J. Low, F.C. Walsh, R. Wills, J. Power Sources 180 (2008) 630.
[7] R.G.A. Wills, J. Collins, D. Stratton-Campbell, C.T.J. Low, D. Pletcher, F.C. Walsh, J. Appl. Electrochem., in press. Q2
[8] J. Collins, D. Stratton-Campbell, X. Li, D. Pletcher, F.C. Walsh, in preparation.
[9] J.P. Carr, N.A. Hampson, Chem. Rev. 72 (1972) 679.
[10] P. Ruetschi, J. Power Sources 2 (78) (1977) 3.
[11] A.T. Kuhn (Ed.), The Electrochemistry of Lead, Academic Press, London, 1979.
[12] A.M. Couper, D. Pletcher, F.C. Walsh, Chem. Rev. 90 (1990) 837.
[13] J.R. Feng, D.C. Johnson, J. Electrochem. Soc. 138 (1991) 3328.
[14] R. Amadelli, A. De Battisti, D.V. Girenko, S.V. Kovalyov, A.B. Velichenko, Electrochim. Acta 46 (2000) 341.
[15] L. Gherardini, P.A. Michaud, M. Panizza, C. Comninellis, N. Vatistas, J. Electrochem. Soc. 148 (2001) D78.
[16] M.E. Herron, D. Pletcher, F.C. Walsh, J. Electroanal. Chem. 332 (1992) 183.
[17] S.E. Doyle, M.E. Herron, K.J. Roberts, J. Robinson, F.C. Walsh, Phase Transitions 39 (1992) 135.
[18] D. Devilliers, M.T. Dinh Thi, E. Mahe, V. Dauriac, N. Lequeux, J. Electroanal. Chem. 573 (2004) 227.
[19] W. Mindt, J. Electrochem. Soc. 116 (1969) 1076.
[20] J.A. Duisman, W.F. Giauque, J. Phys. Chem. 72 (1968) 562.
[21] J.C.G. Thanos, D.W. Wabner, J. Electroanal. Chem. 182 (1985) 25.
[22] N. Munichandraiah, J. Appl. Electrochem. 22 (1992) 825.
[23] A.B. Velichenko, R. Amadelli, A. Benedetti, D.V. Girenko, S.V. Kovalyov, F.I. Danilov, J. Electrochem. Soc. 149 (2002) C445.
[24] D. Linden, T.B. Reddy (Eds.), Handbook of Batteries, McGraw-Hill, New York, 2002.
[25] K. Kinoshita, Electrochemical Oxygen Technology, John Wiley & Sons, New York, 1992.
[26] A.B. Velichenko, R. Amadelli, E.V. Gruzdeva, T.V. Luk'yanenko, F.I. Danilov, J. Power Sources, in press. Q3
[27] International Centre for Diffraction Data Power Diffraction File, ICDD, Philadelphia, PA, card no. 72-2440 for α-PbO_2 and card no. 76-0564 for β-PbO_2, 2001.
[28] A.L. Patterson, Phys. Rev. 56 (1939) 978.
[29] C.T.J. Low, D. Pletcher, F.C. Walsh, Electrochem. Commun., submitted. Q4
[30] R.A. Baker, J. Electrochem. Soc. 109 (1962) 337.
[31] H. Bode, Lead-Acid Batteries, Wiley, New York, 1977.
[32] K. Harris, R.J. Hill, D.A.J. Rand, J. Electrochem. Soc. 131 (1984) 474.

Please cite this article in press as: X. Li, et al., A novel flow battery: A lead acid battery based on an electrolyte with soluble lead(II)—Part VII. Further studies of the lead dioxide positive electrode, Electrochim. Acta (2009), doi:10.1016/j.electacta.2009.03.075